Journal of Materials & Environmental Sustainability Research (2025), 5(2): 1-15
p-ISSN: 2811-1338; e-ISSN: 2811-132X
DOI: https://doi.org/10.55455/jmesr.2025.003

Original Research Paper

Response Surface Optimization of Crystal violet Removal onto Sodium Hydroxide-modified Watermelon Rind

Deborah O. Aderibigbe, Olawale S. Dabo*, Mumeenat O. Olabamiji, Abdur-Rahim A. Giwa

Department of Pure and Applied Chemistry, Ladoke Akintola University of Technology, P.M.B. 4000, Ogbomoso, Nigeria

*Corresponding author: sdolawale41@pgschool.lautech.edu.ng (Olawale S. Dabo)

Received: January 23, 2025; Received in revised form: March 27, 2025; Accepted: March 29, 2025; Published: July 31, 2025

Abstract

The increasing global demand for water and the widespread contamination of water bodies by harmful dyes necessitate sustainable solutions. This study investigates the potential of sodium hydroxide modified-watermelon rind as an adsorbent for Crystal violet (CV) sequestration from aqueous media. Batch adsorption tests were conducted to examine the effects of pH, adsorbent dosage, initial dye concentration, temperature, and contact time on adsorption efficiency. Adsorbent properties analysis was done using pH-point-of-zero charge, Fourier Transform Infrared Spectroscopy and Scanning Electron Microscopy. Analysis of factors' effects and interactions on the adsorption process was conducted using Historical Data Design in Response Surface Methodology. Experimental data were fitted into four isotherm model (Freundlich, Temkin, Dubinin-Raduskevich and Redlich-Peterson). The order of their fitness based on their coefficient of determination, chi-square and RMSE values was Freundlich > Dubinin-Raduskevich > Redlich-Peterson > Temkin. The maximum adsorption capacity of the adsorbent was found to be 76.05 mg/g. The Pseudo-second order kinetic model represented the best fit for the adsorbent. Response Surface Methodology (RSM) results showed that among the four factors (pH, concentration, contact and dosage) examined, only concentration and dosage were significant terms for the adsorption process both having p values <0.05.

Keywords: Crystal violet; Eco-friendly; Optimization; Sustainable adsorbent; Watermelon rind

DOI: 10.55455/jmesr.2025.003

1. Introduction

The Triphenylmethane group of dye is one of the most widely applied synthetic dye across various industries. This class of synthetic dye have found diverse applications in industries such as textile, food and cosmetics, leather, etc. This group of dye have high degree of solubility in water due to their chemical structure which comprises of three aryl groups bonded to a central carbon atom (Mani et al. 2016; Mota et al. 2021).

Crystal violet (CV) is a prominent member of the triphenylmethane class of dye and has been utilized in diverse areas of human endeavours such as the medical field as a 'biological stain', and due to its intense colouration, CV is an important dye frequently used in the textile industry for dyeing several materials such as wool and cotton. In the paper industry, CV serves as pigment for pen and ink for printer (Mani et al. 2016; IARC 2022). Despite its widespread application, there have been several side effects and environmental issues arising from CV usage and disposal into the eco-system. It has the capacity to cause irritation in the eyes, skin and digestive tract. It also disrupts cell division suggesting it is carcinogenic (Mirza and Ahmad 2020). As a result of this, wastewater containing CV must be adequately treated before discharge into the environment. Several

methods have been employed in treating wastewater containing CV, however adsorption using commercial activated carbon stands out as a pivotal and extensively employed technology in wastewater treatment due to its simplicity and cost-effectiveness (Revellame et al. 2020).

The high cost of producing commercial activated carbon has led to several attempt to seek for alternative materials with high adsorption capacity. While previous studies have explored various agro-waste-based adsorbents for CV removal, limited research has focused on NaOH modification of watermelon rind, despite its potential to enhance adsorption capacity through surface activation (Jasper et al. 2020; El Jery et al. 2024). Watermelon (*Citrullus lanatus*), a widely consumed fruit, has a rind that constitutes about one-third of its total mass and is often discarded as waste. Watermelon rind (WMR) is a lignocellulosic material rich in cellulose, pectin, and carotenoids, with functional groups that enhance its adsorption capacity for pollutants. Several studies have investigated the adsorption potential of WMR and its derivatives (Rezagholizade-Shirvan et al. 2023; Wei et al. 2023).

However, most of these studies rely on the one-factor-at-a-time (OFAT) approach, which varies a single parameter while keeping others constant. This method fails to capture interaction effects between variables, leading to sub-optimal process efficiency and limited scalability. Additionally, many adsorption studies still use linearized isotherm models, which may introduce inaccuracies in parameter estimation (Satapathy and Das 2014; El-Shafie et al. 2021)

In other to enhance the adsorption capacity of WMR, NaOH modification was chosen due to its ability to increase surface area, porosity, and the availability of functional groups through lignin disruption. NaOH is also preferred over other chemical treatments due to its environmentally friendly nature, mild corrosiveness, minimal required dosage, and cost-efficiency compared to other options such as KOH (Kusuma et al. 2023). The novelty of the NaOH-modified watermelon rind (N-WMR) lies in its enhanced adsorption capacity, which surpasses many conventional agro-waste adsorbents, making it a more efficient option for dye removal. In this study, the adsorption of Crystal violet onto NaOH-modified Watermelon rind was studied and the optimization of the adsorption process was carried out using Historical Data Design (HDD) in Response Surface Methodology (RSM).

2. Materials and Methods

2.1 Reagents and Materials Used

Analytical grade reagents were used throughout this study and were used without purification. Crystal violet (Colour index (Lot No: 130510; λ_{max} 584 nm; molecular weight 364.91 g/mol) was supplied by Kem Light Laboratories, Mumbai, India. Sodium hydroxide and formaldehyde were used for the adsorbent modification. Stock solution of CV was prepared by weighing accurately 1.0 g of the dye into 1000 ml volumetric flask and made up to the mark with distilled water. Working solutions (10 – 250 mg/L) of the dye were prepared from the stock.

2.2 Preparation of NaOH Modified Watermelon Rind (N-WMR)

Watermelon rind used in this work was procured from Wazo Market Ogbomoso, Oyo State Nigeria. It was chopped into small pieces and was washed several times with distilled water to ensure the removal of dirt and other foreign materials. It was then oven-dried at 75 ^{o}C for 24 hours.

The preparation of the NaOH modified adsorbent followed a two-step process. Firstly, 30 g of the dried watermelon rind was accurately weighed and 375 mL of 2% formaldehyde was added to it. This was placed in the oven at 50 ^{o}C for 4 hours with periodic stirring. Excess formaldehyde was removed by washing with distilled water. It was then oven-dried at 75 ^{o}C for 4 hours. Formaldehyde treatment was applied to polymerize and immobilize soluble substances and colour components within the lignocellulosic matrix, thereby enhancing the structural stability of the adsorbent and preventing excessive leaching during subsequent modification (Olajire et al. 2014). Modification with NaOH then followed by the addition of 450 mL 0.2 M NaOH to the watermelon rind pre-treated with 2% formaldehyde. The mixture was thoroughly stirred and placed in the oven at 50 ^{o}C for

24 hours. Excess NaOH was drained and the material was washed several times with distilled water to a neutral pH. It was then dried at 75 °C for 12 hours, sieved into different particle sizes and stored in airtight containers as NaOH modified watermelon rind adsorbent (N-WMR).

2.3 Characterization of NaOH Modified Watermelon Rind (N-WMR)

Surface morphological studies of N-WMR was carried out using Scanning Electron Microscope (Field Emission Scanning Electron Microscopy, FE-SEM JSM- 7800 F, Joel Ltd). The adsorbent was coated with gold before SEM analysis. Functional groups examination was carried out within the wavelength range of 4000 – 400 cm^{-1} using Fourier Transform Infrared Spectroscopy (FT-IR Tracer-100-Shimadzu). KBr pellets were mixed with the adsorbent prior to the analysis and pH-point of zero charge (pHpzc) determination was carried out by addition of 0.1 g N-WMR to 45 mL solution of 0.1 M NaCl whose pH had been pre-adjusted (2 - 12) with 0.1 M HCl or NaOH.

2.4 Batch Adsorption Studies

Batch adsorption experiments were conducted to evaluate the effects of adsorbent dosage (0.05 – 0.6 g), contact time (10 – 420 min), initial dye concentration (10 – 200 mg/L), temperature (30 – 60 °C), and solution pH (5 – 12) on CV removal. Sample solutions were periodically withdrawn for residual CV concentration determination with the aid of UV–Visible spectrophotometer at the maximum wavelength of 584 nm. The adsorption capacity qe of CV onto N-WMR at equilibrium is shown in equation (1) below:

$$q_e = \frac{C_o - C_e}{M} \times V \quad (1)$$

Where: q_e = quantity of CV adsorbed (mg/g) at equilibrium
C_o = the initial concentration of CV (mg/L);
M = dosage of adsorbent (g);
V = volume of adsorbate solution (L)

2.5 Effect of solution pH, N-WMR Dosage, Temperature, Contact time and Initial CV Concentration

The effect of solution pH was studied by varying the pH between 5 – 12. The solution pH was adjusted using 0.1 M NaOH or HCl with adsorbent dosage (0.1 g), temperature (30 °C), and initial CV concentration (50 mg/L) kept constant. To examine the effect of N-WMR dosage, 40 mL of CV solution (50 mg/L) was added to 100 mL glass bottles containing varying adsorbent doses (0.05 – 0.6 g) and shaken until equilibrium. The effect of Temperature was examined by maintaining 0.1 g of N-WMR at different temperatures (30 – 60 °C). Contact time studies were conducted at intervals (10 – 420 min), while initial CV concentration effects were studied between 10 – 200 mg/L, with 0.1 g adsorbent and 30 °C held constant.

2.6 Adsorption Isotherm Models

Adsorption isotherm models reveal crucial information on the partition of adsorbate and adsorbent at equilibrium. Several models such as Langmuir, Freundlich and Temkins have been employed in studying these relationships (Jawad et al. 2019). In this study, Freundlich, Temkin, Dubinin-Raduskevich and Redlich-Peterson were used (**Table 1**). Origin 2024 64-bit Academic software (OriginLab Corporation, Northampton, MA, USA) was used in fitting the models used in this study.

2.7 Adsorption Kinetic Models

Data from the experiment were subjected to two popular kinetic models (**Table 1**) in order to reveal further insights into the amount of solute retained at constant pH, adsorbent dosage and temperature (George et al. 2018).

Table 1. Isotherm and kinetic models adopted for the removal of CV onto N-WMR

Isotherm models	**Non-linear form**	**Non-linear plot**	**Parameters**
Redlich-Peterson	$q_e = \frac{K_{RP}C_e}{a_R Ce^R + 1}$	q_e vs C_e	K_{RP} = Redlich-Peterson isotherm constant (Lg) and a_R is the constant in L/mg
Freundlich	$q_e = K_f C_e^{1/n}$	q_e vs C_e	K_f = Freundlich adsorption constant (mg/g) related to adsorption capacity and 1/n = Strength of adsorption
Temkin	$q_e = \frac{RT}{b_T} \ln A_T C_e$	q_e vs C_e	b_T = Temkin constant related to the heat of adsorption (j/mol) and A_T = Temkin isotherm constant (L/g)
Dubinin-Raduskevich	$q_e = q_m e^{-K\varepsilon^2}$	q_e vs C_e	q_m = Adsorption capacity (mg/g), ε = Polanyi potential
Kinetic Models			
Pseudo First Order	$q_t = q_e (1 - e^{-k_1 t})$	q_e vs t	K_1 = Pseudo-first rate constant and qe and qt are the amount of CV adsorbed at equilibrium and at time *t* respectively
Pseudo Second Order	$q_t = q_e - e = \frac{q_t}{tk_2 q_e}$	q_e vs t	K_2 = Pseudo-second rate constant and qe and qt are the amount of CV adsorbed at equilibrium and at time *t* respectively

2.8 Adsorption Thermodynamics

Thermodynamic parameters such as change in entropy (ΔS°), change in enthalpy (ΔH°) and Gibb's free energy (ΔG°) were evaluated using Van't Hoff equation as shown below:

$$\Delta G = -RTlnK_o \quad (2)$$

Where,

$$k_0 = \frac{q_e}{C_e} \quad (3)$$

Also,

$$\Delta G = \Delta H - T\Delta S \quad (4)$$

Therefore

$$\Delta H - T\Delta S = -RTlnK_0 \quad (5)$$

Linear form;

$$lnk_o = \frac{\Delta S}{R} - \frac{\Delta H}{RT} \quad (6)$$

Where, ΔG°= Gibb's free energy (kJmol^{-1}), ΔH° = change in enthalpy (kJmol^{-1}), ΔS° = Change in entropy (kJmol^{-1}K^{-1}), T = Temperature (K), R = Universal gas constant and K_o = Adsorption distribution coefficient. The values of ΔH° and ΔS° are evaluated from the intercept and slope of the graph of InK_o against 1/T while ΔG° is evaluated from equation (4) above (Merija et al. 2023).

2.9 Optimization Study

Historical data design (HDD) in Design Expert v13 (Stat Ease Inc., Minneapolis, USA) was used in this study. HDD has found wide application in several areas such as optimization of the effect of sorbate-sorbent interphase on the adsorption of pesticides (Ighalo et al. 2020) and modelling and optimization of sand minimum transport condition in pipeline multiphase flow (Salam et al. 2018). Experimental data was inputted into Design Expert v13 under HDD for modelling and analysis. Four factors which was designated as operational variables (pH, initial CV concentration, contact time, and N-WMR dosage) was inputted and the number of responses was set at one (qe). The factors assigned and response is shown in **Table 2**. A total of 29 experimental runs were performed from the design.

Table 2. Summary of the Historical Data Design (HDD) used for the optimization of CV

Factor	Name	Unit	Minimum	Maximum
A	pH	-	5	11
B	Dosage	g	0.05	0.6
C	Concentration	mg/L	10	200
D	Contact time	minutes	10	180
Response	Adsorption capacity	mg/g	3.28	78.25

3. Results and Discussion

3.1 Characterization of Adsorbent

pH-point-of-zero Charge (pHpzc)

The surface chemistry of an adsorbent plays a vital role for effective removal of contaminants in aqueous medium. The pH-point of zero charge offers the opportunity to gain insight into the net surface charge of adsorbent (Abegunde et al. 2024). The pHpzc of N-WMR was noted to be 8.5 as seen in **Figure 1**. This implies that at this pH, N-WMR surface possess a neutral charge while above this pH value the surface becomes negatively charged which could enhance the removal of cationic species, but at pH values lower than this pHpzc, N-WMR surface becomes positively charged (Loulidi et al. 2020).

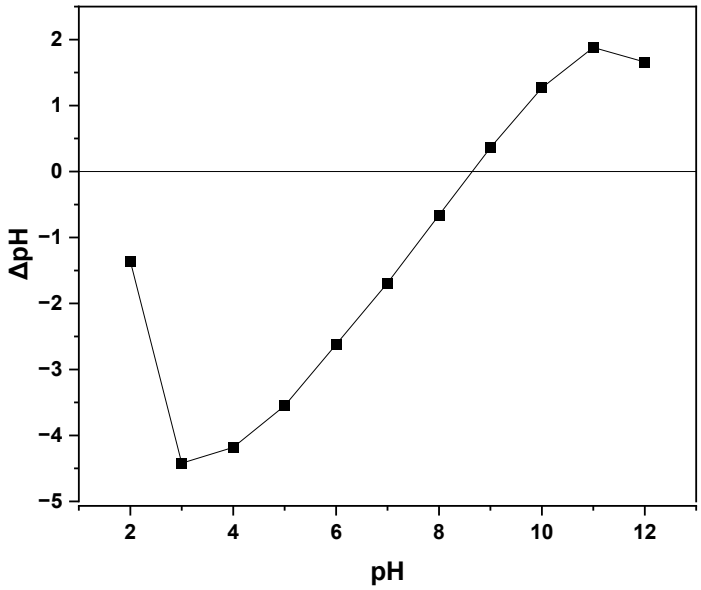

Figure 1: pH_{pzc} of N-WMR

Fourier transform Infrared Spectroscopy (FTIR) of N-WMR

The FTIR spectrum of N-WMR prior to adsorption reveals the presence of various functional groups that could aid the adsorption of CV onto N-WMR (**Figure 2**). Specifically, the well-defined peak at 1681 cm^{-1} could be assigned to the C=C stretching vibrations of alkene while the peak at 501 cm^{-1} could be as a result of C-I stretching vibration. Peaks at 1080, 1421 and 2341 cm^{-1} corresponds to =C-H out of plane bending vibration of alkenes or S=O of sulfoxides, C-H bending vibration of alkanes and C≡C stretching of alkynes or C≡N of nitriles respectively. The band observed at 2480 cm^{-1} could be ascribed to the S-H stretching vibration of mercaptans. After the adsorption of CV onto N-WMR, notable changes were noted in the FTIR spectrum, categorically, there were the

appearances of new peaks at 1301 and 1741 cm^{-1} which could ascribed to S=O of sulfones and C=O stretching vibration of aldehyde. New bands ascribed N-H stretching of amines also appeared at 3201 cm^{-1} (Pavia et al. 2013).

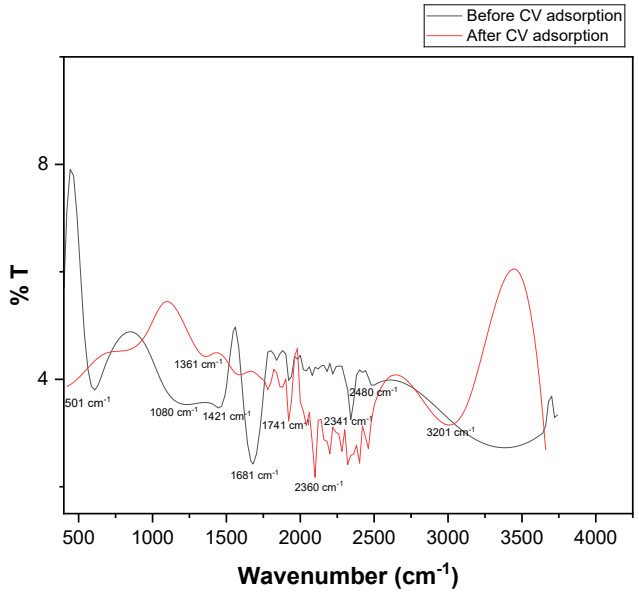

Figure 2: FTIR spectra of N-WMR before and after CV adsorption

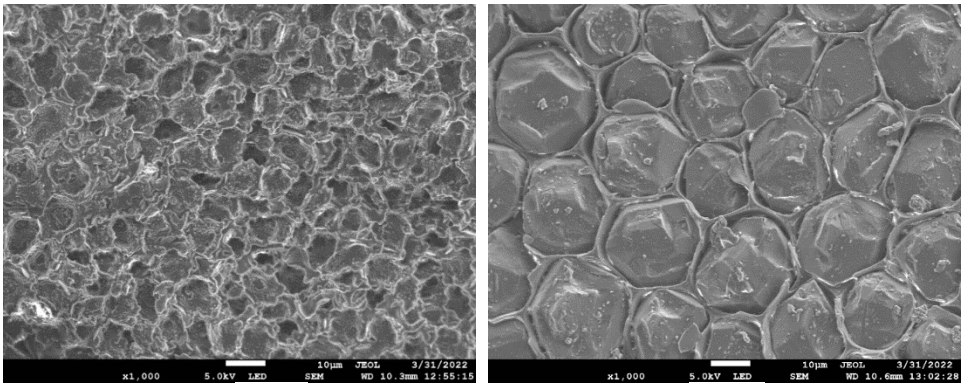

Figure 3: SEM images of N-WMR (a) before CV adsorption and (b) after CV adsorption

3.2 Batch Adsorption Studies

Effect of Solution pH

The solution pH plays a significant role in the adsorption process, variations in the pH of the medium could lead to changes in the net surface charge of the adsorbent and the degree of ionization of adsorbate molecules (Fouda-Mbanga et al. 2024). The effect of solution pH on CV adsorption onto N-WMR is presented in **Figure 4a**. It can be seen from the results that increase in solution pH from 5 - 12 led to marginal decrease in adsorption capacity from 19.72 to 19.56 mg/g. Hence, the optimum pH was 5. The marginal decrease noted when the solution pH was raised could be as a result of competition for active sites between CV molecules and surplus hydroxyl ions (OH^-). Sen et al. (2024) reported similar results on the adsorption of CV onto adsorbents prepared from royal palm leaf sheath. They recorded the optimum pH at 6 and noted reduced adsorption at pH higher than 6. Cheruiyot and co-workers also reported similar findings in their study of the adsorption Crystal violet onto coffee husks. They recorded the optimum pH at 3 (Cheruiyot et al. 2019). In addition, the elevated adsorption of N-WMR at pH values below its point of zero charge (pH_{pzc}) can be attributed to the adsorbent's modification which reduces the material's reliance pH-driven electrostatic interactions, instead facilitating adsorption through alternative

mechanism such as hydrogen bonding and van der Waals forces. Zayed et al. (2023), observed enhanced adsorption of Methylene blue (MB) onto sugar beet leaf-derived adsorbents at pH 2-5, suggesting that non-electrostatic interactions played a dominant role in driving adsorption onto the adsorbents.

Effect of Contact Time

Contact time is a critical factor in determining the equilibrium kinetics of the adsorption process. By investigating this vital operational parameter, researchers can assess the stability and efficiency of the overall adsorption system (Oloo et al. 2020). The uptake of CV as a function of time was studied and the result is presented in **Figure 4b.** The adsorption of CV onto N-WMR occurred rapidly within the first ten minutes and afterward proceeded gradually till attainment of equilibrium at 240 minutes. Similar finding was also reported by Homagai et al. (2020).

Effect of Initial CV Concentration

The initial dye concentration plays a crucial role in the adsorption process, significantly impacting dye removal efficiency and also influences the availability of active binding sites on the adsorbent surface, thereby affecting overall effectiveness of the process (Rapo and Tonk 2021). The adsorption of CV onto N-WMR was studied between 10 – 200 mg/L and the result is illustrated in **Figure 4c**. It can be seen from the results that the adsorption capacity rose sharply from 3.85 to 78.25 mg/g with increase in concentration. This can be attributed to the increased intensity in driving force as the initial concentration was raised thereby overcoming resistance and facilitating increased adsorption rates (Zamouche et al. 2020). Al-Shehri et al. (2021) reported similar finding on the adsorption of CV onto NaOH-activated *Aerva javanica* leaf.

Effect of Adsorbent Dosage

The effectiveness of an adsorbent for removal of contaminants hinges on the availability of binding sites. Moreover, the quantity of adsorbent used also impact the economic viability of the overall treatment process (Hambisa et al. 2022). CV adsorption onto N-WMR was studied as a function adsorbent dosage (between 0.05 – 0.6 g) and the result is shown in **Figure 4d**. The quantity of CV adsorbed onto N-WMR decreased sharply as the adsorbent dosage was raised. This could be as a result of saturation of active sites or particle agglomeration at heightened dosage leading to binding site blockage thus diminishing adsorption capacity (Kamdod and Kumar 2022). Elella et al. (2024) has reported similar findings.

Effect of Temperature

Temperature is a pivotal parameter that significantly influences the adsorption process. The effect of temperature on CV removal was studied between 30 – 60 ^{o}C and as observed in the result in **Figure 4e**, increase in temperature led to increase in adsorption capacity until 40 ^{o}C and afterwards, there was a slight decline in quantity adsorbed which shows that the overall reaction is exothermic which may be ascribed to reduction in interaction forces between CV molecules and the reactive sites of the adsorbent (Budnyak et al. 2020).

3.3 Adsorption Isotherm Models

Adsorption isotherm models reveals crucial information on the partition of adsorbate and adsorbent at equilibrium (Jawad et al. 2019). The adsorption of CV onto N-WMR was investigated using four isotherm models: Freundlich, Temkin, Dubinin-Raduskevich and Redlich-Peterson. The fitness of each model was evaluated based on the coefficient of determination (R^2), root mean square error (RMSE) and the reduced chi-square (χ^2) (**Figure 5a** and **Table 3**). Among the models, the Freundlich isotherm exhibited the best fit, as evidenced by its high R^2 value (0.9967) and low RMSE and χ^2 values. This suggests that adsorption occurs on a heterogeneous surface with varying energy sites, characteristic of lignocellulosic adsorbents like N-WMR. The Freundlich constant K_f (12.33 mg/g) indicates a relatively high adsorption capacity, while the parameter 1/n (0.81) falls within the 0–1 range, confirming favourable adsorption (Al-Ghouti & Da'ana, 2020). Adaramaja et al. (2024), examined the efficiency of thermally modified nanocrystalline snail shell adsorbent for methylene blue removal, among the different isotherm model employed, the Freundlich model provided the best fit for the experimental data. The good fit of the Freundlich model implies that adsorption is multilayered, where dye molecules first occupy the

most energetically favourable sites, followed by progressively weaker interactions at other sites. This can be attributed to the diverse functional groups present in N-WMR, including hydroxyl, carboxyl, and pectin-derived moieties, which facilitate different adsorption mechanisms such as electrostatic interactions and hydrogen bonding (Al-Ghouti & Da'ana, 2020). Although the Dubinin-Radushkevich (R^2 = 0.9358) and Redlich-Peterson (R^2 = 0.9358) models also showed moderate correlation, they did not surpass Freundlich in capturing the adsorption behaviour. The maximum adsorption capacity (Q_m) from the Dubinin-Radushkevich model was 76.05 mg/g, reinforcing the effectiveness of N-WMR as an adsorbent for CV removal.

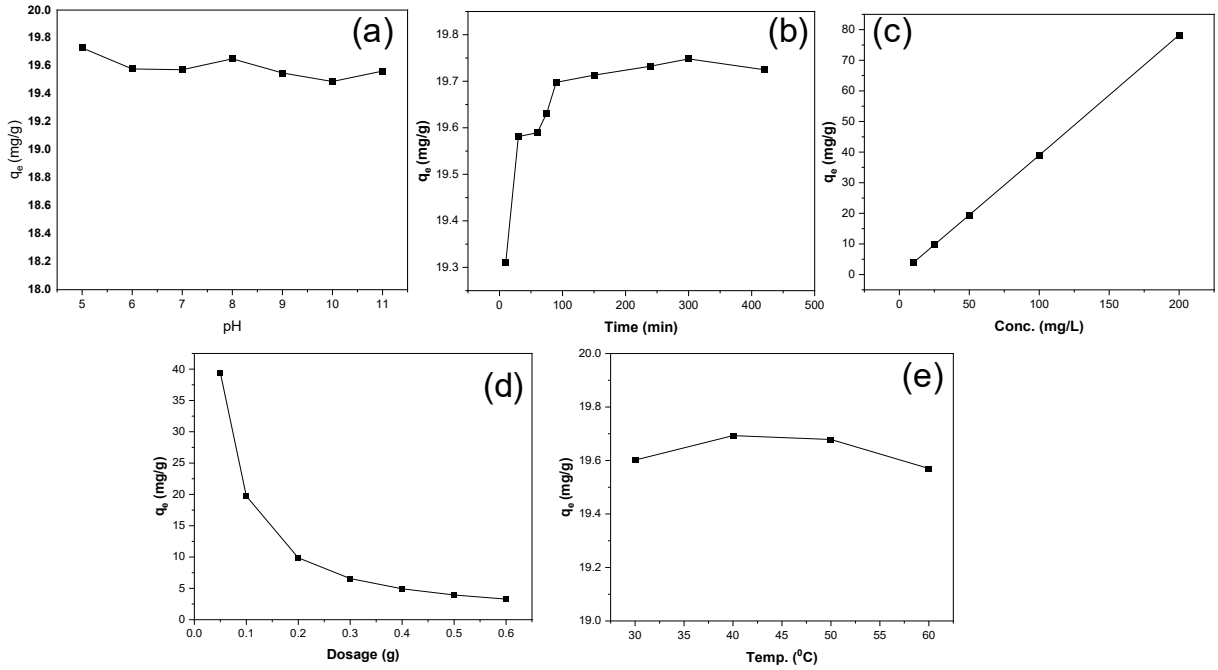

Figure 4. Influence of (a) solution pH (b) contact time (c) initial CV concentration (d) N-WMR dosage and (e) temperature on CV removal onto N-WMR

3.4 Adsorption Kinetic Models

Two widely adopted kinetic model namely: the Pseudo-first order (PFO) and Pseudo-second order (PSO) were employed in examining the adsorption of CV onto N-WMR. Evaluation of each model was based on the coefficient of determination (R^2), root mean square error (RMSE) and the reduced chi-square (χ^2) (**Figure 5b and Table 4**). The superior fit of the PSO model (R^2 = 0.9443), as indicated by a higher coefficient of determination and lower error values, suggests that the adsorption process is primarily controlled by chemisorption. Chemisorption involves electron sharing or transfer between the CV molecules and the functional groups on the N-WMR surface, leading to stronger and more specific interactions compared to physisorption (George et al. 2018). The NaOH modification of watermelon rind likely introduced functional groups, which play a crucial role in chemical bonding during the adsorption process. These functional groups can interact with CV molecules through mechanisms such as electrostatic attraction, ion exchange, and hydrogen bonding. Additionally, the presence of nitrogen-containing groups in CV molecules may facilitate strong electrostatic interactions with the negatively charged sites on the N-WMR surface, further supporting the chemisorption mechanism. Previous studies have reported similar adsorption behaviour, where PSO kinetics were observed in the adsorption of cationic dyes onto chemically modified lignocellulosic adsorbents (Abbas et al. 2021; Sen et al. 2024).

3.5 Adsorption Thermodynamics

Thermodynamics parameters such as such as change in entropy (ΔS^o), Gibbs free energy (ΔG^o), and change in enthalpy (ΔH^o) which are vital variables in assessing the feasibility and spontaneity of the adsorption process were evaluated from the experimental data using the Van't Hoff plot (ln k_o vs 1/T). These parameters are shown in **Table 5.** The negative value obtained for ΔH^o implies that the adsorption process is exothermic while positive

ΔS^o value is an indication of a heightened disorderliness at CV and N-WMR interface (Abubakar et al. 2023). In addition, the negative ΔG^o obtained in this study signifies the spontaneity and the thermodynamic favourability of overall adsorption process (Sen et al. 2024).

Table 3. Isotherm parameters for CV removal onto N-WMR

Isotherm model	Parameters	Values
Temkin	R^2	0.8842
	A_T (L/mg)	1.56
	B_T (J/mol)	32.68
	RMSE	3.36
	χ^2	54.101
Redlich-Peterson	R^2	0.9201
	K_{RP} (Lg)	15.73
	a_R (L/mg)	$1x10^{-4}$
	N	$1x10^{-10}$
	RMSE	5.82
	χ^2	33.92
Freundlich	R^2	0.9967
	K_f (mg/g)	12.33
	1/n	0.81
	RMSE	1.74
	χ^2	3.02
Dubinin-Raduskevich	R^2	0.9358
	Q_m (mg/g)	76.05
	E (kJ/mol)	0.3241
	RMSE	4.879
	χ^2	23.805

Table 4. Kinetics parameters for CV removal onto N-WMR

Isotherm model	Parameters	Values
PFO	R^2	0.7969
	K_1	0.3978
	q_{ecal}	19.6783
	q_{eexp}	19.73
	RMSE	0.0624
	χ^2	0.0039
PSO	R^2	0.9443
	K_2	0.2289
	q_{ecal}	19.72
	q_{ecal}	19.73
	RMSE	0.0327
	χ^2	0.0010

Table 5. Thermodynamic parameters for the adsorption of CV onto N-WMR

Temp. (K)	ΔG° (kJ/mol)	ΔH° (kJ/mol)	ΔS° (kJ/mol/K)
303	-7.51	-3.23	25.54
313	-8.31		
323	-8.59		
333	-8.03		

3.6 Historical Data Design (HDD) Modelling Results

Analysis of Variance (ANOVA)

Based on statistical parameters such as the coefficient of determination R^2, adjusted R^2, and predicted R^2, the modified cubic model represents the best fit in modelling CV onto N-WMR. ANOVA results are shown in **Table 6** and from the results it can be deduced that the cubic model used in this study is significant. A model is considered significant when the p value is less than 0.05 accompanied with a commensurate f value (i.e low p value and high f value) (Rezazadeh et al. 2021). The p value and f values for the adopted cubic model utilized in this study are 0.0001 and 15735 respectively, hence the model is adjudged as significant. The two factors of concentration (B) and dosage (D) were both significant terms both having p values less than 0.0001. pH and time were not significant model terms. And based on the p and f values, concentration is the most significant factor, followed by dosage. The quadratic terms B2 and D2, and cubic terms B3 and D3 were also significant model terms. The coded values obtained from cubic model employed is shown in equation (7) below. Positive and negative signs accompanying each model term signals either antagonistic or synergistic effects respectively on CV adsorption onto N-WMR. The strong positive coefficient for concentration (B = 36.0826) indicates enhanced adsorption with increasing CV concentration. In contrast, dosage (D = -3.8169) shows an antagonistic effect at higher levels, likely due to site aggregation. The quadratic cubic term (D^3 = -10.1209) further confirm this trend. Minimal effects of pH (A = -0.0897415) and time (C = 0.0387412) suggest their limited influence on adsorption efficiency (Ma et al. 2021).

$$Q_e = 26.6857 + -0.0897415 * A + 36.0826 * B + 0.0387412 * C + -3.8169 * D + 0.444385 * B^2 + 7.66792 * D^2 + 1.14141 * B^3 + -10.1209 * D^3 \quad (7)$$

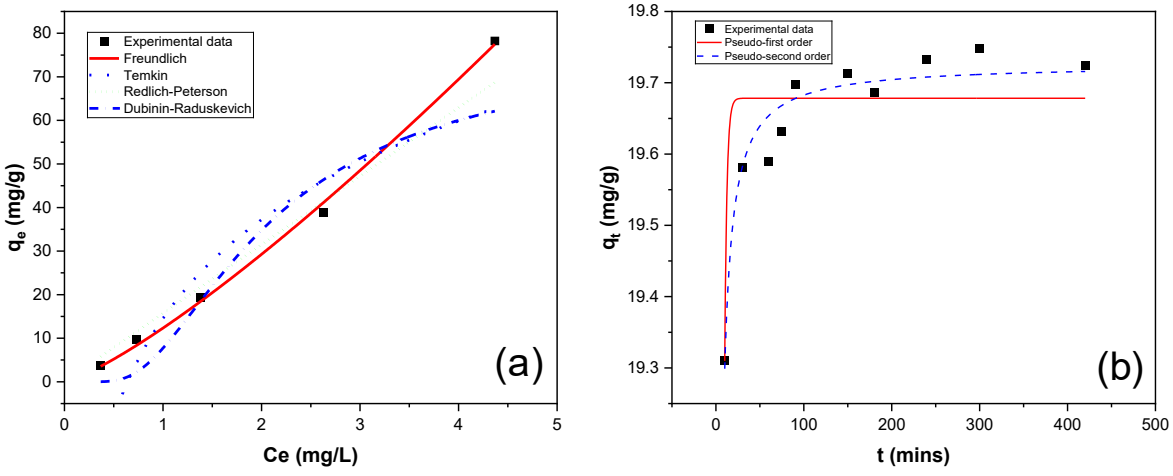

Figure 5. (a) Isotherm and (b) kinetics plots for CV adsorption onto N-WMR

Table 6. ANOVA parameters for the modified cubic model utilized for modelling CV removal

Source	Sum of Squares	Df	Mean Square	F-value	p-value	Verdict
Model	4873.87	8	609.23	26082.79	< 0.0001	Significant
A-pH	0.0349	1	0.0349	1.50	0.2372	
B-Conc	246.66	1	246.66	10560.29	< 0.0001	
C-Time	0.0141	1	0.0141	0.6016	0.4480	
D-Dosage	2.36	1	2.36	100.90	< 0.0001	
B^2	0.1273	1	0.1273	5.45	0.0314	
D^2	9.81	1	9.81	420.12	< 0.0001	
B^3	0.2053	1	0.2053	8.79	0.0083	
D^3	3.74	1	3.74	160.21	< 0.0001	
R^2	0.9999					
Adjusted R^2	0.9999					
Predicted R^2	0.9586					
Residual	0.4204	18	0.0234			
Lack of Fit	0.3591	15	0.0239	1.17	0.5137	not significant

Perturbation Plot for CV Removal onto N-WMR

From the perturbation plot shown in **Figure 6a**, it can clearly be seen that increase in model terms A (pH) and C (time) have no significant effect on the adsorption capacity of N-WMR. However, increase in model term D (dosage) led to steady reduction in the adsorption capacity of N-WMR and increase in term B (concentration) had the most pronounced effect on the adsorption capacity of N-WMR. Model term B had direct proportional relationship on the adsorption capacity (Salam et al. 2024). The predicted versus actual plot displayed in **Figure 6b** also showed that the majority of the data points are well dispersed closely along the straight line which is an indication of the accuracy of the developed model (Ighalo et al. 2020).

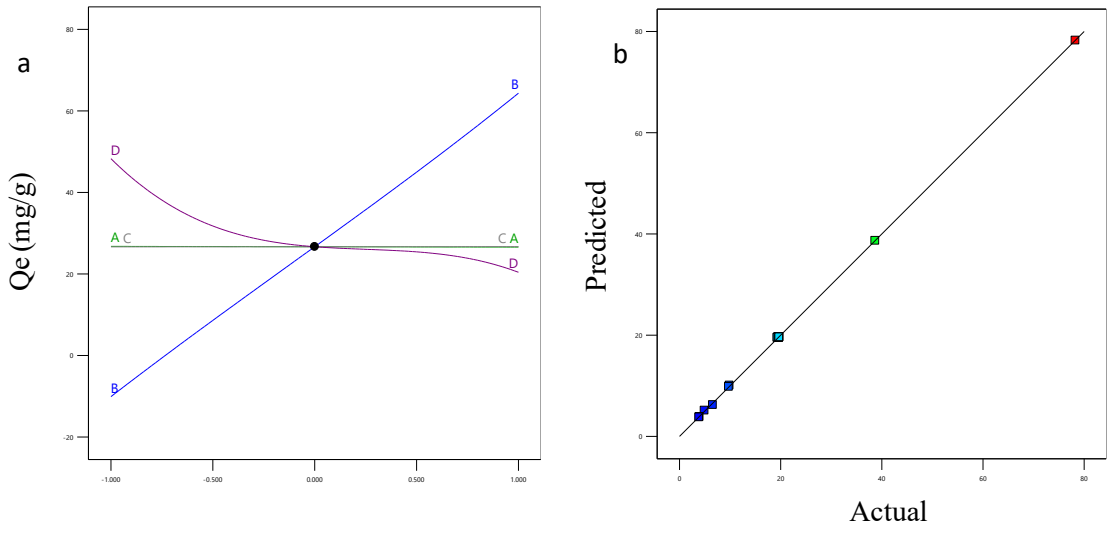

Figure 6. (a) Perturbation plot and (b) Predicted values vs Experimental values plot for CV removal onto N-WMR

4. Conclusion

In conclusion, this study demonstrates that NaOH-modified watermelon rind (N-WMR) is an effective adsorbent for CV removal, achieving a maximum adsorption capacity of 76.05 mg/g. The adsorption process followed the Freundlich isotherm model (R^2 = 0.9967), indicating multilayer adsorption on a heterogeneous surface. Kinetic analysis showed that the process was best described by the Pseudo-second-order model, suggesting chemisorption as the dominant mechanism. Thermodynamic studies confirmed that the adsorption was spontaneous and exothermic. The modified cubic model in RSM provided a significant predictive tool for optimizing adsorption. Future studies should explore real wastewater applications and adsorbent regeneration potential.

Acknowledgement

We appreciate the financial support provided by the *Journal of Materials and Environmental Sustainability Research* for supporting this research through a travel grant to present our findings at the 8th Annual American Chemical Society (ACS) Nigeria International Chapter Symposium, as well as covering the costs of this publication.

Authors' contributions

Conceptualization: A.A Giwa; Methodology: A.A Giwa and D.O. Aderibigbe; Supervision: D.O. Aderibigbe; Benchwork: M.O. Olabamiji; Data curation: A.A Giwa and D.O. Aderibigbe Statistical Modelling: O.S. Dabo; Writing—original draft: O.S Dabo and M.O. Olabamiji; Writing—review & editing: D.O. Aderibigbe

Declaration of Competing Interests

There are no conflicts to declare.

References

Abbas, S., Javeed, T., Zafar, S., Taj, M.B., Ashraf, A.R., & Din, M.I. (2021). Adsorption of crystal violet dye by using a low-cost adsorbent – peanut husk. *Desalination and Water Treatment*, 233:387-398. https://doi.org/10.5004/dwt.2021.27538

Abegunde, S. M., Olasehinde, E. F., & Adebayo, M. A. (2024). Green synthesis of ZnO nanoparticles using Nauclea latifolia fruit extract for adsorption of Congo red. *Hybrid Advances*, *5*, 100164. https://doi.org/10.1016/j.hybadv.2024.100164

Abubakar, H. L., Tijani, J. O., Abdulkareem, A. S., Egbosiuba, T. C., Abdullahi, M., Mustapha, S., & Ajiboye, E. A. (2023). Effective removal of malachite green from local dyeing wastewater using zinc-tungstate based materials. *Heliyon*, *9*(9), e19167. https://doi.org/10.1016/j.heliyon.2023.e19167

Adaramaja, A. A. Bamisaye, A., Abati, S.M., Adegoke, K.A., Adesina, M.O., Ige, A.R., Adeleke. O., Idowu, M.A., Oyebamiji, A.K., and Solomon Bello, O.S. (2024). Thermally modified nanocrystalline snail shell adsorbent for methylene blue sequestration: Equilibrium, kinetic, thermodynamic, artificial intelligence, and DFT studies. *RSC Advances*. **14**, 12703 – 12719.

Al-Ghouti, M. A., and Da'ana, D. A. (2020). Guidelines for the use and interpretation of adsorption isotherm models: A review. *Journal of Hazardous Materials*, **393**, 122383. https://doi.org/10.1016/j.jhazmat.2020.122383

AL-Shehri, H. S., Almudaifer, E., Alorabi, A. Q., Alanazi, H. S., Alkorbi, A. S., & Alharthi, F. A. (2021). Effective adsorption of crystal violet from aqueous solutions with effective adsorbent: Equilibrium, mechanism studies and modeling analysis. *Environmental Pollutants and Bioavailability*, *33*(1), 214–226. https://doi.org/10.1080/26395940.2021.1960199

Budnyak, T. M., Błachnio, M., Slabon, A., Jaworski, A., Tertykh, V. A., Deryło-Marczewska, A., & Marczewski, A. W. (2020). Chitosan Deposited onto Fumed Silica Surface as Sustainable Hybrid Biosorbent for Acid

Orange 8 Dye Capture: Effect of Temperature in Adsorption Equilibrium and Kinetics. *The Journal of Physical Chemistry C*, *124*(28), 15312–15323. https://doi.org/10.1021/acs.jpcc.0c04205

Cheruiyot, G. K., Wanyonyi, W. C., Kiplimo, J. J., & Maina, E. N. (2019). Adsorption of toxic crystal violet dye using coffee husks: Equilibrium, kinetics and thermodynamics study. *Scientific African*, *5*, e00116. https://doi.org/10.1016/j.sciaf.2019.e00116

El Jery, A., Alawamleh, H. S. K., Sami, M. H., Abbas, H. A., Sammen, S. Sh., Ahsan, A., Imteaz, M. A., Shanableh, A., Shafiquzzaman, Md., Osman, H., & Al-Ansari, N. (2024). Isotherms, kinetics and thermodynamic mechanism of methylene blue dye adsorption on synthesized activated carbon. *Scientific Reports*, *14*(1), 970. https://doi.org/10.1038/s41598-023-50937-0

Elella, M. H., Aamer, N., Abdallah, H. M., López-Maldonado, E. A., Mohamed, Y. M. A., El Nazer, H. A., and Mohamed, R. R. (2024). Novel high-efficient adsorbent based on modified gelatin/montmorillonite nanocomposite for removal of malachite green dye. *Scientific Reports*, **14** (1), 1228. https://doi.org/10.1038/s41598-024-51321-2

El-Shafie, A. S., Hassan, S. S., Akther, N., & El-Azazy, M. (2021). Watermelon rinds as cost-efficient adsorbent for acridine orange: A response surface methodological approach. *Environmental Science and Pollution Research*, 30(28), 71554–71573. https://doi.org/10.1007/s11356-021-13652-9

Fouda-Mbanga, B. G., Velempini, T., Pillay, K., & Tywabi-Ngeva, Z. (2024). Heavy metals removals from wastewater and reuse of the metal loaded adsorbents in various applications: A review. *Hybrid Advances*, *6*, 100193. https://doi.org/10.1016/j.hybadv.2024.100193

George, W.K., Emik, S., Ongen, A., Ozcan, H.K and Aydin, S. (2018). Modelling of Adsorption Kinetic Processes—Errors, Theory and Application, *Advanced Sorption Process Applications*, publisher; Intech Open, chapter (10), https://doi.org/10.5772/intechopen.80495

Hambisa, A. A., Regasa, M. B., Ejigu, H. G., & Senbeto, C. B. (2023). Adsorption studies of methyl orange dye removal from aqueous solution using Anchote peel-based agricultural waste adsorbent. *Applied Water Science*, *13*(1), 24. https://doi.org/10.1007/s13201-022-01832-y

Homagai, P. L., Poudel, R., Poudel, S., & Bhattarai, A. (2022). Adsorption and removal of crystal violet dye from aqueous solution by modified rice husk. *Heliyon*, *8*(4), e09261. https://doi.org/10.1016/j.heliyon.2022.e09261

Jasper, E. E., Ajibola, V. O., & Onwuka, J. C. (2020). Nonlinear regression analysis of the sorption of crystal violet and methylene blue from aqueous solutions onto an agro-waste derived activated carbon. *Applied Water Science*, *10*(6), 132. https://doi.org/10.1007/s13201-020-01218-y

Jawad, A. H., Razuan, R., Appaturi, J. N., & Wilson, L. D. (2019). Adsorption and mechanism study for methylene blue dye removal with carbonized watermelon (Citrullus lanatus) rind prepared via one-step liquid phase H_2SO_4 activation. *Surfaces and Interfaces*, *16*, 76–84. https://doi.org/10.1016/j.surfin.2019.04.012

K. S., M., Rahulan, K. M., Sujatha, R. A., & Little Flower, N. A. (2023). Adsorption of hexavalent chromium from water using graphene oxide/zinc molybdate nanocomposite: Study of kinetics and adsorption isotherms. *Frontiers in Energy Research*, *11*, 1139604. https://doi.org/10.3389/fenrg.2023.1139604

Kamdod, A. S., & Pavan Kumar, M. V. (2022). Adsorption of Methylene blue and Methyl orange on tamarind seed activated carbon and its composite with chitosan: Equilibrium and kinetic studies. *Desalination and Water Treatment*, *252*, 408–419. https://doi.org/10.5004/dwt.2022.28270

Kusuma, H. S., Aigbe, U. O., Ukhurebor, K. E., Onyancha, R. B., Okundaye, B., Simbi, I., Ama, O. M., Darmokoesoemo, H., Widyaningrum, B. A., Osibote, O. A., & Balogun, V. A. (2023). Biosorption of methylene blue using clove leaves waste modified with sodium hydroxide. *Results in Chemistry*, 5, 100778. https://doi.org/10.1016/j.rechem.2023.100778

IARC (2022). Gentian violet, leucogentian violet, malachite green, leucomalachite green, and CI Direct Blue 218. IARC Monogr Identif Carcinog Hazards Hum, 129:1–178.

Loulidi, I., Boukhlifi, F., Ouchabi, M., Amar, A., Jabri, M., Kali, A., Chraibi, S., Hadey, C., & Aziz, F. (2020). Adsorption of Crystal Violet onto an Agricultural Waste Residue: Kinetics, Isotherm, Thermodynamics, and Mechanism of Adsorption. *The Scientific World Journal*, *2020*, 1–9. https://doi.org/10.1155/2020/5873521

Ma, C.-M., Yu, T.-J., Yang, C.-H., & Hong, G.-B. (2021). Enhancement of plasticizer adsorption by utilizing a rice bran-derived adsorbent. *Ecotoxicology and Environmental Safety*, *228*, 112972. https://doi.org/10.1016/j.ecoenv.2021.112972

Mani, S., & Bharagava, R. N. (2016). Exposure to Crystal Violet, Its Toxic, Genotoxic and Carcinogenic Effects on Environment and Its Degradation and Detoxification for Environmental Safety. In W. P. De Voogt (Ed.), *Reviews of Environmental Contamination and Toxicology Volume 237* (Vol. 237, pp. 71–104). Springer International Publishing. https://doi.org/10.1007/978-3-319-23573-8_4

Mirza, A., & Ahmad, R. (2020). An efficient sequestration of toxic crystal violet dye from aqueous solution by Alginate/Pectin nanocomposite: A novel and ecofriendly adsorbent. *Groundwater for Sustainable Development*, *11*, 100373. https://doi.org/10.1016/j.gsd.2020.100373

Merija, K.S., Rahulan, K.M., Sujatha, R.A., & Little Flower N.A. (2023), Adsorption of hexavalent chromium from water using graphene oxide/zinc molybdate nanocomposite: Study of kinetics and adsorption isotherms. *Front. Energy Res*. **11**:1139604. https://doi: 10.3389/fenrg.2023.1139604

Ighalo, J.O., Adelodun, A.A., Adeniyi, A.G., & Igwegbe, C.A. (2020). Modelling the Effect of Sorbate-Sorbent Interphase on the Adsorption of Pesticides and Herbicides by Historical Data Design. *Iranian Journal of Energy and Environment*, *11*(4). https://doi.org/10.5829/IJEE.2020.11.04.02

Mota, I. G. C., Neves, R. A. M. D., Nascimento, S. S. D. C., Maciel, B. L. L., Morais, A. H. D. A., & Passos, T. S. (2023). Artificial Dyes: Health Risks and the Need for Revision of International Regulations. *Food Reviews International*, *39*(3), 1578–1593. https://doi.org/10.1080/87559129.2021.1934694

Olajire, A. A., Giwa, A. A., & Bello, I. A. (2014). Competitive adsorption of dye species from aqueous solution onto melon husk in single and ternary dye systems. International Journal of Environmental Science and Technology, 12(3), 939–950. https://doi.org/10.1007/s13762-013-0469-8

Oloo, C. M., Onyari, J. M., Wanyonyi, W. C., Wabomba, J. N., & Muinde, V. M. (2020). Adsorptive removal of hazardous crystal violet dye form aqueous solution using Rhizophora mucronata stem-barks: Equilibrium and kinetics studies. *Environmental Chemistry and Ecotoxicology*, *2*, 64–72. https://doi.org/10.1016/j.enceco.2020.05.001

Pavia, D.L., Lampman, G.M., Kriz, G.S., Vyvyan, J.R. (2013). Introduction to spectroscopy, Fifth Edition. Cengage Learning.

Rápó, E., & Tonk, S. (2021). Factors Affecting Synthetic Dye Adsorption; Desorption Studies: A Review of Results from the Last Five Years (2017–2021). *Molecules*, *26*(17), 5419. https://doi.org/10.3390/molecules26175419

Revellame, E. D., Fortela, D. L., Sharp, W., Hernandez, R., & Zappi, M. E. (2020). Adsorption kinetic modeling using pseudo-first order and pseudo-second order rate laws: A review. *Cleaner Engineering and Technology*, *1*, 100032. https://doi.org/10.1016/j.clet.2020.100032

Rezazadeh, M., Baghdadi, M., Mehrdadi, N., & Ali Abdoli, M. (2020). Adsorption of crystal violet dye by agricultural rice bran waste: Isotherms, kinetics, modeling and influencing factors. *Environmental Engineering Research*. https://doi.org/10.4491/eer.2020.128

Rezagholizade-shirvan, A., Shokri, S., Dadpour, S. M., & Amiryousefi, M. R. (2023). Evaluation of physicochemical, antioxidant, antibacterial activity, and sensory properties of Watermelon Rind Candy. *Heliyon*, 9(6). https://doi.org/10.1016/j.heliyon.2023.e17300

Salam, K. K., Aremu, M. O., Oke, E. O., Babatunde, K. A., Oluwole, T. D., Ibrahim, S. O., & Oke, A. B. (2024). Lignin extraction from sawdust: Optimization of experimental studies, computer-aided simulation and

techno-economic analysis of scale-up process design with uncertainty quantification. *Systems Microbiology and Biomanufacturing*, *4*(2), 750–765. https://doi.org/10.1007/s43393-023-00197-w

Salam, K. K., Arinkoola, A. O., & Aminu, M. D. (2018). Application of Response Surface Methodology (Rsm) for the Modelling and Optimization of Sand Minimum Transport Condition (Mtc) In Pipeline Multiphase Flow. *Petroleum and Coal*, 60(2): 339-348

Satapathy, M. K., & Das, P. (2014). Optimization of crystal violet dye removal using novel soil-silver nanocomposite as nanoadsorbent using response surface methodology. *Journal of Environmental Chemical Engineering*, 2(1), 708–714. https://doi.org/10.1016/j.jece.2013.11.012

Sen, N., Shefa, N. R., Reza, K., Shawon, S. M. A. Z., & Rahman, Md. W. (2024). Adsorption of crystal violet dye from synthetic wastewater by ball-milled royal palm leaf sheath. *Scientific Reports*, *14*(1), 5349. https://doi.org/10.1038/s41598-024-52395-8

Wei, Y., Li, P., Yang, C., Li, X., Yi, D., & Wu, W. (2023). Preparation of porous carbon materials as adsorbent materials from phosphorus-doped watermelon rind. *Water*, 15(13), 2433. https://doi.org/10.3390/w15132433

Zamouche, M., Habib, A., Saaidia, K., & Bencheikh Lehocine, M. (2020). Batch mode for adsorption of crystal violet by cedar cone forest waste. *SN Applied Sciences*, *2*(2), 198. https://doi.org/10.1007/s42452-020-1976-0

Zayed, A. M., Metwally, B. S., Masoud, M. A., Mubarak, M. F., Shendy, H., Petrounias, P., & Abdel Wahed, M. S. M. (2023). Facile synthesis of eco-friendly activated carbon from leaves of sugar beet waste as a superior nonconventional adsorbent for anionic and cationic dyes from aqueous solutions. *Arabian Journal of Chemistry*, *16*(8), 104900. https://doi.org/10.1016/j.arabjc.2023.104900